The single-longitudinal-mode operation of a ridge waveguide laser based on two-dimensional photonic crystals*

Wang Hua-Yong(王华勇) and Xu Xing-Sheng(许兴胜)†

State Key Laboratory of Integrated Optoelectronics, Institute of Semiconductors, Chinese Academy of Sciences, Beijing 100083, *China*

(Received 21 September 2012; revised manuscript received 26 October 2012)

An electrically driven, single-longitudinal-mode GaAs based photonic crystal (PC) ridge waveguide (RWG) laser emitting at around 850 nm is demonstrated. The single-longitudinal-mode lasing characteristic is achieved by introducing the PC to the RWG laser. The triangle PC is etched on both sides of the ridge by photolithography and inductive coupled plasma (ICP) etching. The lasing spectra of the RWG lasers with and without the PC are studied, and the result shows that the PC purifies the longitudinal mode. The power per facet versus current and current–voltage characteristics have also been studied and compared.

Keywords: ridge waveguide laser, photonic crystals, single-longitudinal mode, effective index guided mode

PACS: 42.55.Px, 42.62.Fi **DOI:** 10.1088/1674-1056/22/5/054205

1. Introduction

High light output power, low energy consumption, and low noise edge emitting lasers operating around 850 nm have been widely used in numerous applications such as pump sources, optical sensors, high speed optical interconnection systems, and data communications.[1–5] Single transverse and longitudinal modes are quite necessary when taking into consideration long distance communication, stability of the beam, device size, heat dispersion, and surrounding disturbance. The ridge waveguide (RWG) laser is the simplest and cheapest way to obtain a single fundamental transverse mode owing to its simple structure and easy fabrication. However, the destabilizing hole-burning effect,[6] strain and scattering centers,[7] deteriorate the quality of the longitudinal mode. As a result, the RWG laser is likely to operate with multi-longitudinal modes. Moreover, the number of oscillating modes in high speed modulation tends to increases as a result of the frequency chirp.[8]

The photonic crystals (PCs)[9,10] provide a new method to control the propagation of light. Due to their excellent characteristics such as photonic bandgap (PBG),[11] slow light,[12] and resonance guided mode,[13] they are widely studied for the applications of vertical-cavity surface-emitting laser (VCSEL), light emitting diode (LED), and compact waveguide.[14–17] In our previous studies,[18] we have etched a PC with air holes into the top distributed Bragg reflector (DBR) of a VCSEL emitting at about 850 nm. The PC not only helps to improve the single transverse mode characteristic but also purifies the longitudinal mode of the VCSEL. In this paper, we etch PC holes with a single line defect to make a PC RWG laser, the PC around the ridge plays an important role in purifying the longitudinal mode. This structure is easy to fabricate and well-suited for planar large-scale integration. We employ the PC with lattice constant $a = 5$ μm and air hole radius-to-lattice constant $r/a = 10\%$ to the RWG laser and obtain a single longitudinal mode output.

2. Growth and fabrication

The schematic diagram of the fabricated PC RWG laser is shown in Fig. 1. The epitaxial layers are grown on an n^+ GaAs substrate. The undoped active layer with AlGaAs quantum wells (QWs) separated by a GaAs barrier is grown by metal-organic chemical vapor deposition (MOCVD). The aluminum proportion of AlGaAs is coordinated to obtain the center wavelength of 850 nm. The optical limiting p- and n-type cladding layers are both deposited in AlGaAs material. The RWG is formed by etching PC holes with a single line defect. The effective index difference between the PC hole and the line defect is designed for the transverse mode confinement. The ends of the ridge waveguide are cleaved to form two parallel mirrors, thus forming a Fabry–Pérot resonator. The cavity length is 591 μm. Then an anodic oxide layer is grown upon the RWG as the electrical confinement layer. The electrodes are grown below the n^+ GaAs substrate and upon the AlGaAs electrical confinement layer.

PC triangular holes are formed by photolithography and inductive coupled plasma (ICP) etching. First, the PC pattern with special markers is transferred to the correct location of photoresist, and then the photoresist is used as the mask for etching AlGaAs, and the etching gas is BCl_3/Cl_2. We optimize the gas ratio, pressure, power, bias, and etching time to get the required depth and less air hole defects. The top view of the

*Project supported by the National Natural Science Foundation of China (Grant No. 91121019) and the National Basic Research Program of China (Grant No. 2013CB632105).

†Corresponding author. E-mail: xsxu@semi.ac.cn

© 2013 Chinese Physical Society and IOP Publishing Ltd

PC RWG laser under scanning electron microscopy is shown in Fig. 2. The RWG is composed as a single line defect PC waveguide. To clearly analyze the effect of PC on the RWG laser, a conventional RWG laser without PC is also fabricated for comparison.

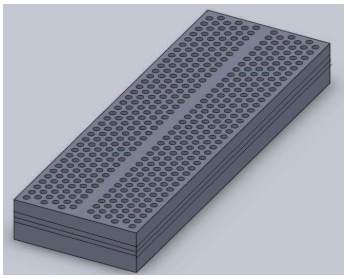


Fig. 1. Schematic diagram of a PC RWG laser.

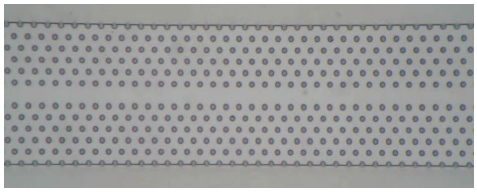


Fig. 2. Top view of the fabricated device.

3. Result and discussion

The two kinds of fabricated lasers are put on a probe station that connects to the anode of a power source for characterization. The power source is a square wave source with frequency 1 kHz, whose duty cycle and magnitude can be tuned. The lattice constant a and the air hole radius-to-lattice constant r/a of the PC are 5 μm and 10%, respectively. Since the longitudinal mode is most important, we firstly study the room temperature lasing spectra at various currents with the frequency of 1 kHz and the duty cycle of 10%. The emission light is coupled into an optical spectrum analyzer (Agilent 86145B) using a multi-mode fiber. The threshold current ($I_{\rm th}$) of the conventional RWG laser is 9 mA. Figures 3(a)–3(c) present the lasing spectra of the conventional RWG laser under several pumping currents. The lasing spectra show that there are two main peaks and a mode competence between the two peaks exists. Figure 3(a) shows that the longer wavelength has a higher lasing peak under driven current $1.1I_{\rm th}$, while the mode at the shorter wavelength begins to dominate under pumping current $1.3I_{\rm th}$ in Fig. 3(b). After increasing the current further to $1.9I_{\rm th}$, the longer wavelength will take the lead again, as shown in Fig. 3(c).

Figures 4(a)–4(c) present the lasing spectra of the PC RWG laser under several driven currents. The threshold current of the PC RWG laser is 13 mA, which is higher than that of the conventional RWG laser. Figure 4(a) presents the lasing spectrum just above the threshold current ($1.1I_{\rm th}$), which shows a single longitudinal

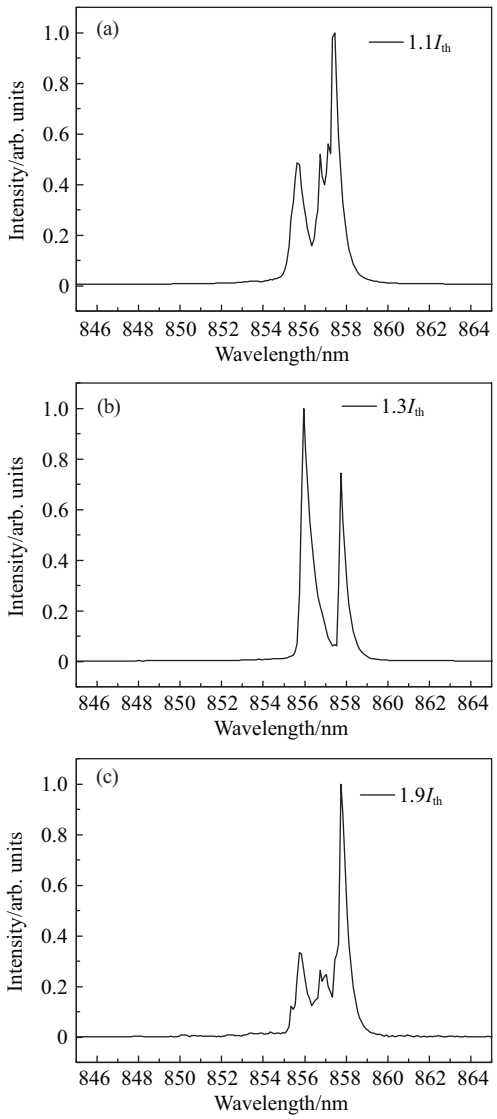


Fig. 3. Lasing spectra of the conventional RWG laser under driven currents: (a) $1.1I_{\rm th}$, (b) $1.3I_{\rm th}$, and (c) $1.9I_{\rm th}$.

mode at around 851.14 nm. However, multi-modes are observed under the current of $1.4I_{\rm th}$ (not shown). Further increasing the current to $1.6I_{\rm th}$, as depicted in Fig. 4(b), a single longitudinal mode appears again. This phenomenon may be explained as follows. As the homogeneous broadening of the optical gain increases at current-induced high temperatures, lasing-mode photons come not only from the energetically resonant QW but also from other non-resonant QWs that lie within the homogeneous broadening, so the multi-modes appear at $1.4I_{\rm th}$. When the current is increased to $1.6I_{\rm th}$, the center wavelength of photons moves from 851.14 nm to 850.99 nm, which is the center wavelength of the neighboring mode at $1.4I_{\rm th}$, so a single-longitudinal mode appears again at $1.6I_{\rm th}$. When the current is increased to $1.8I_{\rm th}$, the multi-mode characteristics will appear again, as depicted in Fig. 4(c). From the lasing spectra at various currents, it can be found that the PC RWG laser shows the single longitudinal mode characteristic when the current is in the ranges from $1.07I_{\rm th}$ to $1.15I_{\rm th}$ and from $1.60I_{\rm th}$ to $1.69I_{\rm th}$. Moreover, the linewidth is also

suppressed as shown in the laser spectrum. The full width at half maximum (FWHM) of the conventional RWG laser is 0.39 nm under the current of $1.6I_{th}$ according to the Lorentz fitting analysis, however, the FWHM of the PC RWG laser is only 0.19 nm. From the lasing spectra, a blue shift is found for the PC RWG laser comparing with the conventional one. The blue shift makes the laser beam closer to the designed 850 nm. The lasing spectral comparison proves that the PC RWG can control and purify the longitudinal mode. The mode purification is attributed to the optical loss or gain modulated by the PC hole.

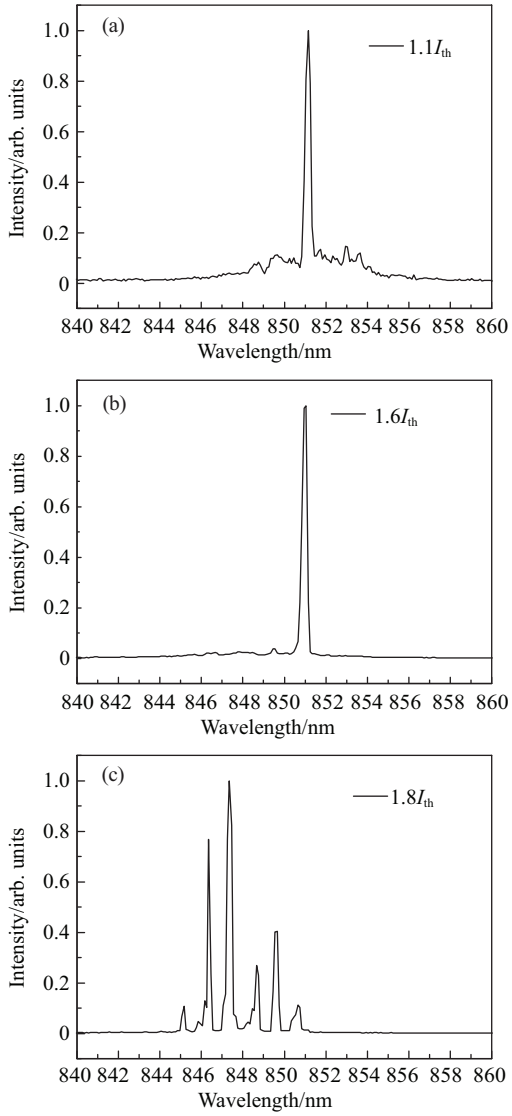


Fig. 4. Lasing spectra of the PC RWG laser under driven currents: (a) $1.1I_{th}$, (b) $1.6I_{th}$, and (c) $1.8I_{th}$.

We have also studied the lasing spectra with different source duty cycles. The spectra of the conventional RWG laser show that there are 2–4 peaks and a mode competence between these peaks exists in different duty cycles. When the duty cycle is as small as 5%, which is shown in Fig. 5(a), the longest wavelength of four main wavelengths has the highest lasing peak. However, the mode at the shorter wavelength begins to dominate with the duty cycle of 10% in Fig. 5(b). After increasing the duty cycle to 20%, the longer wavelength will take the lead again, as shown in Fig. 5(c). After increasing the duty cycle further to 50%, the laser will cease lasing.

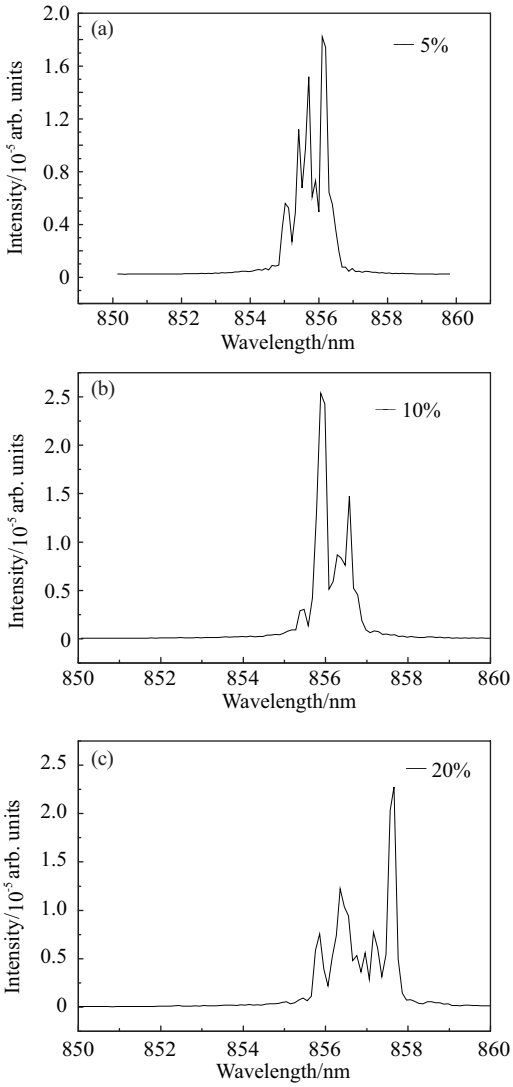


Fig. 5. Lasing spectra of the conventional RWG laser with different source duty cycles: (a) 5%, (b) 10%, (c) 20%.

The spectra of the PC RWG laser with different source duty cycles are shown in Figs. 6(a)–6(c). The PC RWG laser stably operates in the single longitudinal mode without mode competition with the duty cycle from 5% to 15%. Similar to the conventional RWG laser, the PC RWG will cease lasing when the duty cycle is increased to 30%. According to the spectra of the PC RWG laser in different duty cycles, we also find a red shift from 852.58 nm to 852.90 nm when the duty cycle is increased from 5% to 15%. The phenomenon of no lasing and the red shift of spectrum for the increasing duty cycle are attributed to the thermal effect.

Driven by the voltage source with frequency 1 kHz and 10% duty cycle, the power per facet versus current (P–I) and the current versus voltage (I–V) characteristics of the conven-

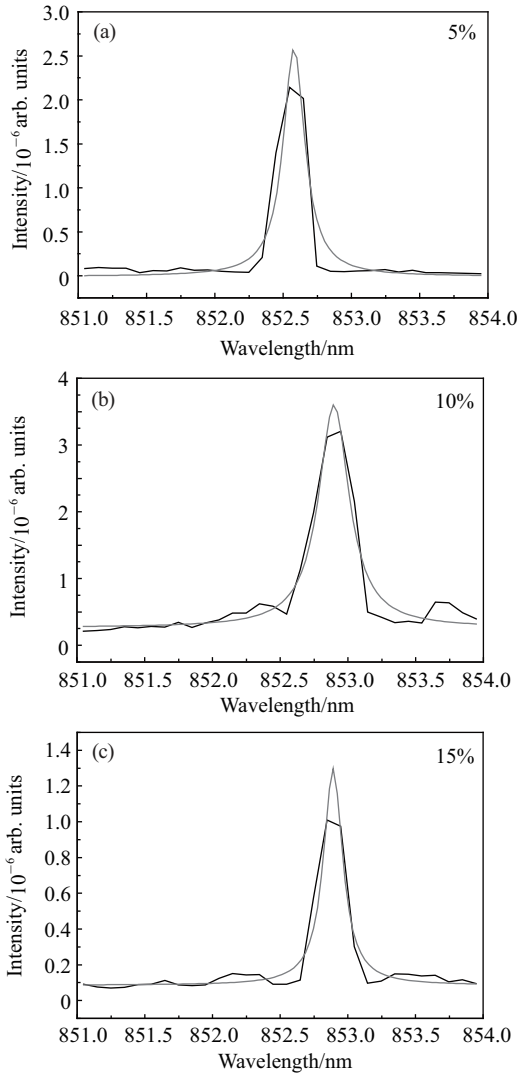


Fig. 6. Lasing spectra of the PC RWG laser with different source duty cycles: (a) 5%, (b) 10%, (c) 15%. Gray lines are Lorentz fitting functions.

tional RWG laser at room temperature are tested and shown in Fig. 7(a). This figure shows that the threshold current I_{th} is 9 mA. The figure also shows that the differential series resistance is approximately 270 Ω and the laser emits maximum output power per facet of 1.64 mW at 33 mA. The power slope efficiency is from 0.03 W/A to 0.05 W/A for current from 9 mA to 20 mA. Figure 7(b) shows the *P*–*I* and *I*–*V* curves of the PC RWG laser. The measurement is also carried out at room temperature. The threshold current is 13 mA, which is higher than that of the conventional RWG laser because the etched PC around the waveguide increases the series resistance. The PC RWG laser emits maximum output power per facet of 0.54 mW at 23 mA. The maximum light output is merely one third of the conventional RWG laser. The lower output power is mainly due to the loss caused by the etched PC holes. The efficiency of the single longitudinal mode PC RWG laser can be improved by varying the lattice constant and the air-hole radius of the PC. In nowadays etching systems, larger lattice constant and air-hole radius will bring lower damage of materials, thus improving the efficiency. However, as the lattice constant increases, some properties of the PC, such as photonic band gap and slow light, will disappear or become weak at short wavelength. Specially, there exist parameters with which the efficiency of the PC can reach the maximum. Our goal is to find these lattice constant and air-hole radius. To reach the goal, we should simulate the optical field and the optical mode of the PC RWG laser with different lattice constants and different air-hole radii by numerical simulation method to get a high efficiency. At the same time, optimizing the dry etching condition to get lower damage of the materials. In Fig. 7(b), the power slope efficiency of PC RWG laser is above 0.05 W/A for 13–20 mA.

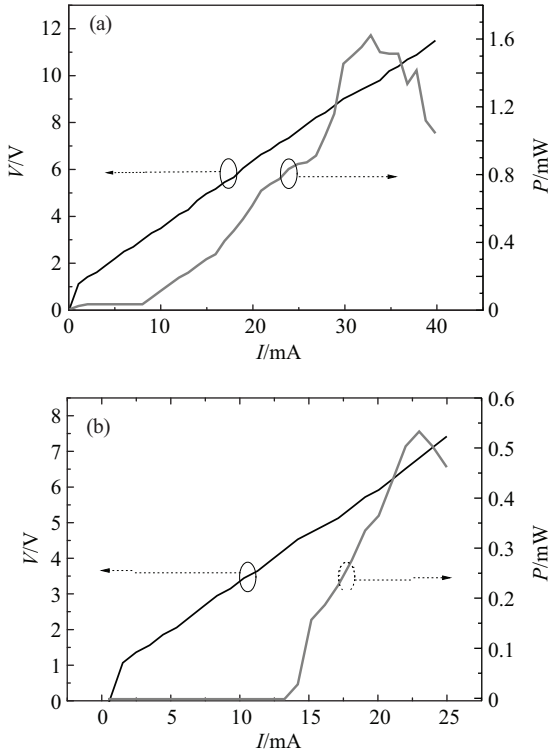


Fig. 7. Power per facet *P*–*I* and *I*–*V* curves of RWG lasers (a) without PC and (b) with PC.

We have tested the lateral mode in our experiments. The result shows that the far field patterns of the RWG lasers with and without the PC are almost the same. The divergence angles of the RWG lasers with and without the PC under the same pulsed operation (15 mA) are 9.50° and 10.98°, respectively. This result shows that the etching PC is somewhat beneficial to achieve a low divergence angle beam.

It is believed that DFB-like guided mode and effective index guided mode are two main mechanisms of PC to select the laser mode. For the DFB-like guided mode, the PC acting as a second-order DFB enhances the light–matter interaction and thus provides an easy and accurate way of controlling the wavelength of the laser.[19] The lattice constant of the PC in DFB-like guided mode is comparable to the wavelength

($L/l < 1$), however, in our work, the lattice constant is rather large ($L/l = 5.88$), so the mechanism for DFB-like guided mode does not work. For the effective index guided mode, light is confined in the central core due to the total internal reflection caused by the index contrast between the central core and the effective surrounding cladding formed by the periodic structure. This effect is like that of the photonic crystal fiber. To further investigate the effective index characteristics of the PC, the 2D plane wave expansion (PWE) algorithm is used.[20] The refractivity indexes of the slab and the hole are 3.6 and 1, which correspond approximately to GaAs and air, respectively. The lattice constant a and the air hole radius-to-lattice constant r/a of the PC are 5 μm and 10%, respectively. For the wavelength $\lambda = 850$ nm used in experiment, the effective index of the waveguide is calculated to be $n_{\text{eff}} = 3.49$. The refractive index contrast is used to confine the light in the evanescent area and purifies the longitudinal mode, which is similar to the effect of PC to VCSEL in our previous studies.[18]

4. Conclusion

We fabricate and characterize an electrically pumped, single longitudinal mode RWG laser emitting at around 850 nm by etching the PC holes with a single line defect. This structure is easy to fabricate and well-suited for planar large-scale integration. By comparing its *P–I*, *I–V* characteristics and lasing spectra with those of the conventional RWG laser, we confirm that etching PC into RWG laser improves the single longitudinal mode characteristic. The single longitudinal mode arises from the index contrast produced by the PC. Etching PC into RWG laser supplies a simple method to control the longitudinal mode, which is also well suitable for large scale planar integration.

References

[1] Shigihara K, Nagai Y, Karakida S, Takami A, Kokubo Y, Matsubara H and Kakimoto S 1999 *IEEE J. Quantum Electron.* **27** 1537
[2] Werle P, Slemr F, Maurer K, Kormann R, Mücke R and Jänker B 2002 *Opt. Lasers Eng.* **37** 101
[3] Van Steenberge G, Hendrickx B, Bosman E, Van Erps J, Thienpont H and Van Daele P 2006 *IEEE Photonics Technol. Lett.* **18** 1106
[4] Wong Y M, Muehlner D J, Faudskar C C, Buchholz D B, Fishteyn M, Brandner J L, Parzygnat W J, Morgan R A, Mullally T, Leibenguth R E, Guth G D, Focht M W, Glogovsky K G, Zilko J L, Gates J V, Anthony P J, Tyrone B H Jr, Ireland T J, Lewis D H Jr, Smith D F, Nati S F, Lewis D K, Rogers D L, Aispain H A, Gowda S M, Walker S G, Kwark Y H, Bates R J S, Kuchta D M and Crow J D 1995 *J. Lightwave Technol.* **13** 995
[5] Goedgebuer J P, Porte H and Hamel A 1987 *IEEE J. Quantum Electron.* **23** 1135
[6] Schmitt-Rink S, Chemla D S and Haug H 1988 *Phys. Rev. B* **37** 941
[7] Peters F H and Cassidy D T 1991 *Appl. Opt.* **30** 1036
[8] Kishino K, Aoki S and Suematsu Y 1982 *IEEE J. Quantum Electron.* **18** 343
[9] Yablonovitch E 1987 *Phys. Rev. Lett.* **58** 2059
[10] John S 1987 *Phys. Rev. Lett.* **58** 2486
[11] Noda S, Tomoda K, Yamamoto N and Chutinan A 2000 *Science* **289** 604
[12] Vlasov Y A, O'Boyle M, HamannH F and McNab S J 2006 *Nature* **438** 65
[13] Crozier K B, Lousse V, Kilic O, Kim S, Fan S and Solgaard O 2006 *Phys. Rev. B* **73** 115126
[14] Yokouchi N, Danner A J and Choquette K D 2003 *IEEE J. Sel. Top. Quantum Electron.* **9** 1439
[15] Kim J Y, Kwon M K, Park S J, Kim S H and Lee K D 2010 *Appl. Phys. Lett.* **96** 251103
[16] Takeda H and John S 2008 *Phys. Rev. A* **78** 023804
[17] Ren C, Cheng L F, Kang F, Gan L, Zhang D Z and Li Z Y 2012 *Chin. Phys. B* **21** 104210
[18] Xu X S, Wang C X, Song Q, Du W, Hu H Y, Zhao Z M, Lu L, Kan Q and Chen H D 2007 *Chin. Sci. Bull.* **52** 2473
[19] Larrue A, Bouchard O, Monmayrant A, Gauthier-Lafaye O, Bonnefont S, Arnoult A, Dubreuil P and Lozes-Dupuy F 2008 *IEEE Photonics Technol. Lett.* **20** 2120
[20] Ho K M, Chan C T and Soukoulis C M 1990 *Phys. Rev. Lett.* **65** 3152